Supplementary Materials for

# Fatigue behavior of freestanding nickel-molybdenum-tungsten thin films with high-density planar faults

JungHun Park, Yuhyun Park, Sunkun Choi, Zhuo Feng Lee, and Gi-Dong Sim*

*Department of Mechanical Engineering, Korea Advanced Institute of Science and Technology 291, Daehak-ro, Yuseong-gu, Daejeon 34141, Republic of Korea*

* Corresponding author

E-mail address: gdsim@kaist.ac.kr

Load-displacement profiles of nickel-molybdenum-tungsten (Ni-Mo-W) thin films

The digital image correlation (DIC) method utilized in uniaxial tensile testing could not be extended to tension-tension cyclic loading. This limits the tracking of plastic strain evolution under stress-controlled fatigue tests (Fig. S1(a)), so instead load-displacement profiles of fatigue-tested Ni-Mo-W thin films were extracted (Fig. S1(b)). The applied load was normalized by Ni-Mo-W's ultimate tensile strength, and the displacement was normalized by the gauge length of the dog-bone specimen for convenience. The profiles for both as-deposited and annealed thin films show a constant slope throughout the test, indicating no direct signs of cyclic hardening of softening. The profiles shown in Fig. S1(b) were consistent for both as-deposited and annealed Ni-Mo-W thin films, regardless of the number of cycles tested.

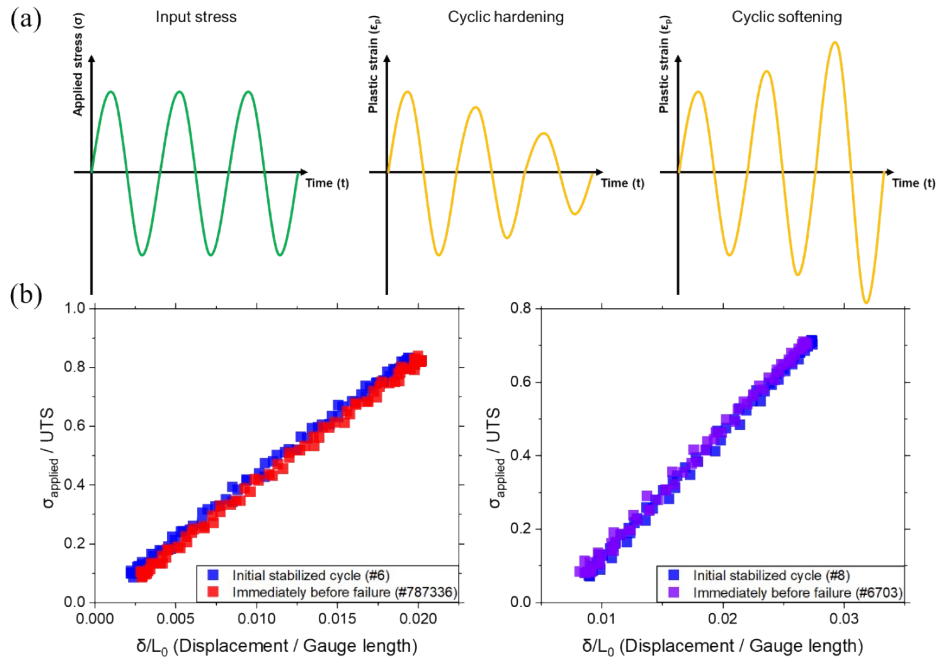


**Fig. S1** (a) Plastic strain profiles under stress-controlled cyclic hardening and softening. (b) Normalized load-displacement profiles of as-deposited (left) and annealed (right) Ni-Mo-W thin films.

Nanocrystalline (nc) and ultrafine-grained (ufg) Ni, nc Ni-based alloys, and nanotwinned (nt) Cu-based metals

All films introduced and juxtaposed in Fig. 6, Results of the manuscript are listed below along with their stress-life (S-N) curves [S1–10]. The description for each sample is written in the following format: material type (author's name; d, λ), where d is the grain size and λ is the twin boundary (TB) spacing.

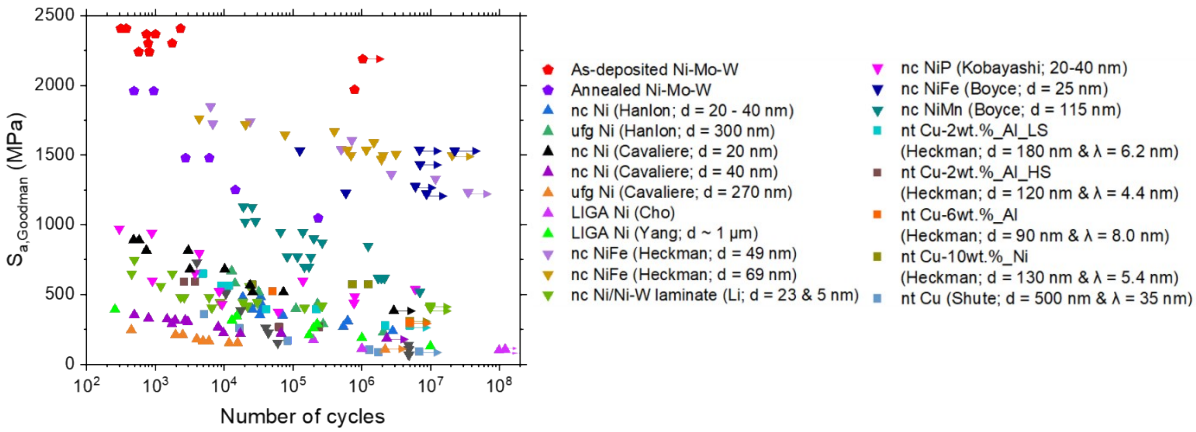


**Fig. S2** S-N curves of all fatigue-tested materials in the Results section of the manuscript. The stress level is expressed as the Goodman stress amplitude to be consistent with the data presented in the manuscript.

Consideration about the effect of residual stress on the fatigue strengths of Ni-Mo-W thin films

Tensile residual stress of the metallic thin film is another factor that may drastically reduce the fatigue strength by aggravating the stress concentration effect [S11]. The residual stresses of as-deposited and annealed Ni-Mo-W films obtained through membrane deflection experiment (MDE) [S12,13] were indeed tensile (+ 430 and + 791 MPa, respectively; Fig. S3), but this should not affect the mechanical properties obtained from micro-mechanical testing. The mounted freestanding thin films are first deliberately buckled by having a compressive displacement applied. Conducting a uniaxial tensile test at this state ensures that the tensile residual stress is fully relieved, and the load increases steeply when the film is fully stretched. Fatigue tests are carried out at the displacement at which the load level increases sharply under tensile loading – i.e. when the film is fully stretched without tensile residual stress.

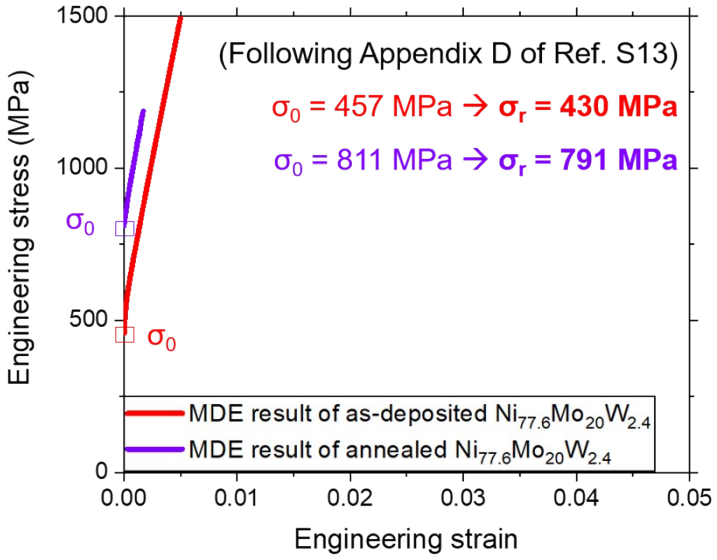


**Fig. S3** Tensile response of as-deposited and annealed Ni-Mo-W thin films obtained by MDE. The y-intercept stress ($\sigma_0$) was used to obtain the final residual stress.

More on the GB characteristics of as-deposited Ni-Mo-W thin films

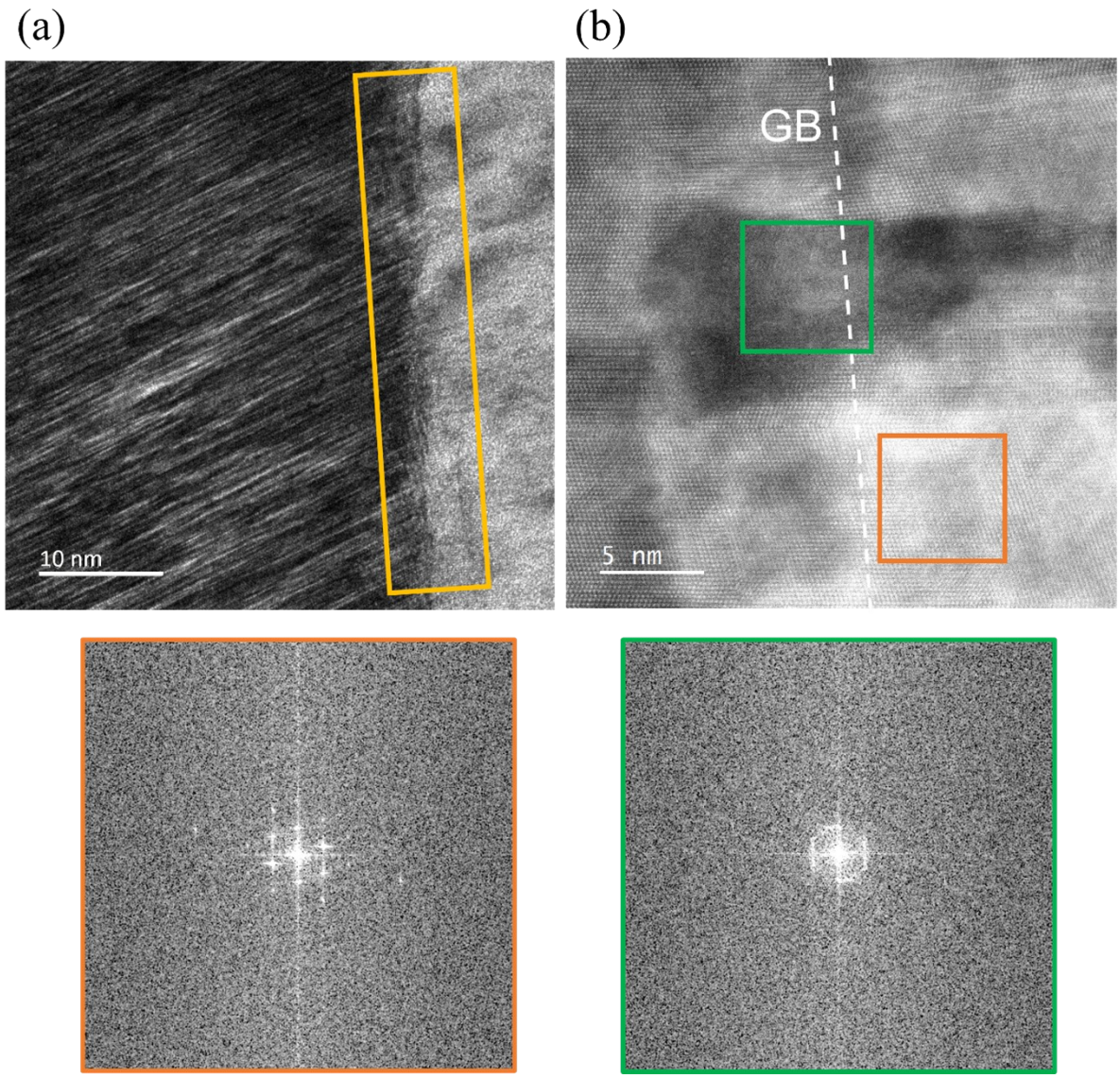


**Fig. S4** (a) a band-like structure along the GB of as-deposited Ni-Mo-W thin film. (b) a spherical aberration-corrected (Cs-corrected) scanning TEM image of an amorphous phase and FFT patterns of a crystalline region (orange square) and an amorphous region (green square).

In-plane STEM-EDS analysis of annealed Ni-Mo-W thin films

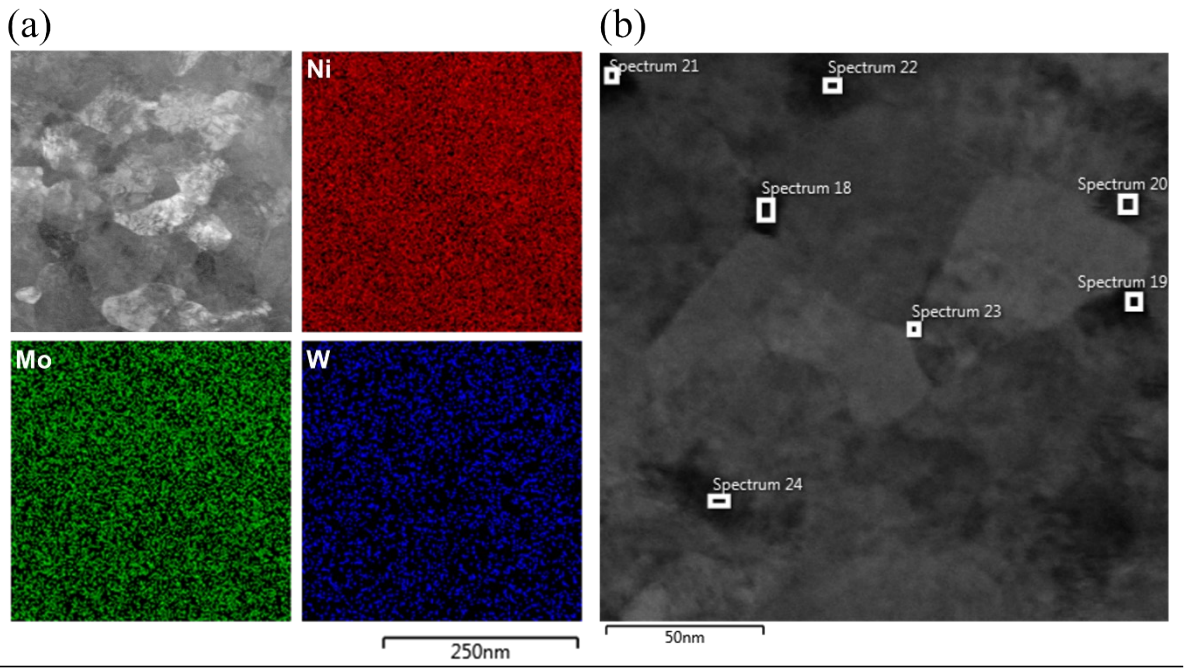


**Figure S5** (a) In-plane STEM-EDS map of annealed Ni-Mo-W thin film (left). An example of in-plane micrograph used for point EDS, and the chemical compositions of selected grains (right).

**Table S1** Chemical compositions of annealed Ni-Mo-W films at the selected points in Fig. S5(b).

| Spectrum number | Ni (at.%) | Mo (at.%) | W (at.%) |
|---|---|---|---|
| 18 | 78.63 | 18.15 | 3.22 |
| 19 | 78.47 | 18.60 | 2.92 |
| 20 | 76.66 | 20.94 | 2.40 |
| 21 | 76.01 | 21.06 | 2.93 |
| 22 | 76.83 | 19.99 | 3.18 |
| 23 | 76.89 | 19.99 | 3.11 |
| 24 | 77.47 | 19.80 | 2.73 |

## References


[S1] T. Hanlon, Y. N. Kwon and S. Suresh, *Scr Mater*, 2003, **49**, 675–680.

[S2] P. Cavaliere, *Int J Fatigue*, 2009, **31**, 1476–1489.

[S3] H. S. Cho, K. J. Hemker, K. Lian and J. Goettert, *Technical Digest. MEMS 2002 IEEE International Conference*.

[S4] Y. Yang, B. I. Imasogie, S. M. Allameh, B. Boyce, K. Lian, J. Lou and W. O. Soboyejo, *Materials Science and Engineering A*, 2007, **444**, 39–50.

[S5] N. M. Heckman, H. A. Padilla, J. R. Michael, C. M. Barr, B. G. Clark, K. Hattar and B. L. Boyce, *Int J Fatigue*, 2020, **134.** DOI:10.1016/j.ijfatigue.2020.105472.

[S6] S. Kobayashi, A. Kamata and T. Watanabe, in *Journal of Physics: Conference Series*, Institute of Physics Publishing, 2010, vol. 240.

[S7] B. L. Boyce and H. A. Padilla, *Metall Mater Trans A Phys Metall Mater Sci*, 2011, **42**, 1793–1804.

[S8] M. Y. Li, Z. X. Wang, B. Zhang, F. Liang, X. M. Luo and G. P. Zhang, *Scr Mater*, 2023, **222**, DOI:10.1016/j.scriptamat.2022.114995.

[S9] N. M. Heckman, M. F. Berwind, C. Eberl and A. M. Hodge, *Acta Mater*, 2018, **144**, 138–144.

[S10] C. J. Shute, B. D. Myers, S. Xie, S. Y. Li, T. W. Barbee, A. M. Hodge and J. R. Weertman, *Acta Mater*, 2011, **59**, 4569–4577.

[S11] G. A. Webster and A. N. Ezeilo, International Journal of Fatigue, 2001, **23**, 375-383

[S12] H. D. Espinosa, B. C. Prorok and M. Fischer, *A methodology for determining mechanical properties of freestanding thin ÿlms and MEMS materials*, 2003, vol. 51.

[S13] H. Kim, J.-H. Choi, Y. Park, S. Choi and G.-D. Sim, J Mech Phys Solids, 2023, **173**, DOI:10.1016/j.jmps.2023.105209.